$1/\omega$ Flux Noise and Dynamical Critical Properties of Two-Dimensional XY Models

P. H. E. Tiesinga,[1,*] T. J. Hagenaars,[1,3] J. E. van Himbergen,[1] and Jorge V. José[2]
[1]*Instituut voor Theoretische Fysica, Princetonplein 5, Postbus 80006, 3508 TA Utrecht, The Netherlands*
[2]*Physics Department and Center for the Interdisciplinary Research on Complex Systems, Northeastern University, Boston, Massachusetts 02115*
[3]*Institut für Theoretische Physik, Universität Würzburg, Am Hubland, 97074 Würzburg, Germany*
(Received 22 August 1996)

We have numerically studied the dynamic correlation functions in thermodynamic equilibrium of two-dimensional O(2) symmetry models with either bond [resistively shunted Josephson (RSJ)] or site [time-dependent Ginsburg-Landau (TDGL)] dissipation as a function of temperature T. We find that above the critical temperature the frequency dependent flux noise $S_\Phi(\omega) \sim |1 + (\omega/\Omega)^2|^{-\alpha(T)/2}$, with $0.85 \leq \alpha(\mathrm{TDGL})(T) \leq 0.95$ and $1.17 \leq \alpha(\mathrm{RSJ})(T) \leq 1.27$, while the dynamic critical exponents $z(\mathrm{TDGL}) \sim 2.0$ and $z(\mathrm{RSJ}) \sim 0.9$. Contrary to expectation the TDGL results are in closer agreement with the experiments in Josephson-junction arrays by Shaw *et al.* [Phys. Rev. Lett. **76**, 2551 (1996)] than those from the RSJ model. [S0031-9007(96)02206-5]

PACS numbers: 74.20.–z, 64.60.Fr, 74.40.+k, 74.50.+r

There is a general theoretical consensus that the equilibrium critical properties of two-dimensional Abelian symmetry statistical mechanical models are properly described by the Berezinskii-Kosterlitz-Thouless (BKT) theory [1,2]. The theory is based on the idea that at low temperatures there are thermally excited vortex-antivortex pairs that unbind just above the BKT critical temperature. Experimental tests have for the most part been indirect, in out of equilibrium conditions. Successful comparisons of the BKT predictions to experiment were initially carried out in superfluid helium [3] and in superconducting films [4]. Later measurements on Josephson-junction arrays (JJA) yielded current-voltage characteristics [5], and dynamic impedance [6] results that also agree with the BKT theory. To explain the experiments, the static BKT scenario was heuristically extended to nonequilibrium situations [7]. One of the basic tenets of the dynamical BKT extensions is that vortices move *diffusively* with binding and unbinding of vortex pairs under the action of the external drive. Further phenomenological modifications to the dynamic extension of the BKT theory, which reduced the number of fitting parameters, have led to better correspondence to some of the experimental results on superconductors [8].

A very recent flux noise SQUID experiment by Shaw *et al.* [9] on proximity effect JJA provided a direct experimental test of the *equilibrium* BKT theory, at $T_{\mathrm{BKT}} < T$ [10]. They found the flux noise to be white at the lowest frequencies, and proportional to $1/\omega^\alpha$, with $\alpha \approx 1$, at intermediate ones rather than the $1/\omega^2$ expected by the phenomenological theories [7,8]. They also carried out a dynamical scaling analysis of the noise function for different temperatures, which yielded a dynamical exponent of $z \sim 2$. An earlier, less extensive, JJA experiment by Lerch *et al.* [11] found a $1/\omega$ behavior for the $T < T_{\mathrm{BKT}}$ regime, without the white noise frequency region. In this Letter we concentrate on the $T_{\mathrm{BKT}} < T$ regime. We show that by numerically calculating quantities *closely* related to those measured in [9] we do get good agreement with their α and z results for a site dissipation model defined below [12].

There are two models that have been considered to study the arrays. One is the resistively shunted Josephson (RSJ) array model and the other is related to the time-dependent Ginsburg-Landau (TDGL) model. The RSJ model is constructed from the elementary RSJ equations for single Josephson junctions that form the array units, plus Kirchhoff's current conservation conditions at each lattice site. The JJA-RSJ model has been successful in explaining, for example, the experimental giant Shapiro steps that arise when the JJA is driven by a dc + ac current [13]. The TDGL model is an alternative dynamical model that has been used to describe the general critical dynamical properties of the XY model [14] and also some aspects of JJA behavior, including its flux noise [15,16]. An important theoretical question is then to ascertain which model is best to describe the experimental noise results. To find out, we have studied the flux noise and dynamical scaling properties for both models. We do indeed find that the flux noise is anomalous in both cases, but the TDGL results appear to be closer to the experimental ones. We find that the vortices do not move independently but in a sea of vortex clusters that modify their diffusive properties.

The equation of motion for both models can be written in the general Langevin equation form,

$$\partial_t \theta(\mathbf{r}, t) = \sum_{\mathbf{r}'} \left(\Gamma(\mathbf{r}, \mathbf{r}') \frac{\partial H[\theta]}{\partial \theta(\mathbf{r}', t)} + W(\mathbf{r}, \mathbf{r}', t) \right). \quad (1)$$

Here $\theta(\mathbf{r}, t)$ is the phase of the order parameter of the superconducting island at site $\mathbf{r}$; $H[\theta] = E_J \cos[\theta(\mathbf{r}', t) - \theta(\mathbf{r}, t)]$ is the Hamiltonian bond energy, with E_J the Josephson coupling, and

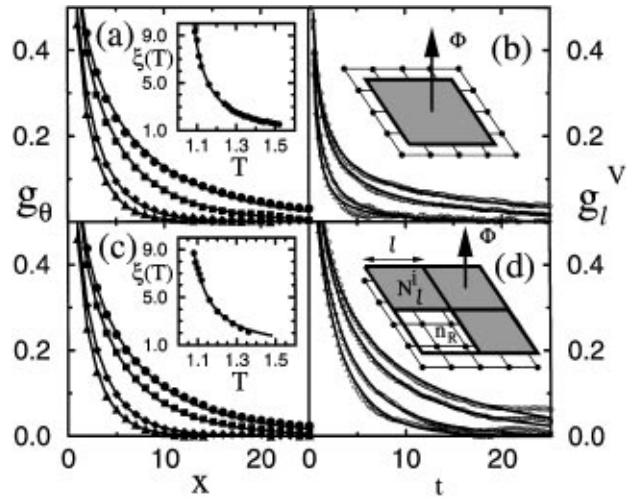

FIG. 1. Results from simulations of a 64×64 array with PBC. Phase correlation functions $g_\theta(x)$ obtained from TDGL (a) and RSJ (c) simulations. The different curves correspond to $T = 1.08$ (○), $T = 1.12$ (squares), $T = 1.24$ (diamonds), and $T = 1.32$ (△). The continuous lines are fits to Eq. (3). Insets to (a) and (c) give the $\xi(T)$ results for TDGL and RSJ dynamics, with the continuous lines fits to the BKT form given in Eq. (4), respectively. In (b) and (d) we plot $g_\ell^V(t)$ for $\ell = 32$. The temperatures and notation is the same as in (a) and (c). The solid lines are fits to Eq. (5).

$W(\mathbf{r}, t; \mathbf{r}', t')$ the noise function. The RSJ model has $\Gamma_{\mathrm{RSJ}}(\mathbf{r}, \mathbf{r}') \equiv \Gamma G(\mathbf{r}, \mathbf{r}')$. In our units $\Gamma = 1$. $G(\mathbf{r}, \mathbf{r}')$, the two-dimensional inverse lattice Laplacian, arises from the fact that the currents in the array are conserved at each lattice site. The dissipation here is present in the junctions between the superconducting islands. The random noise function $W_{\mathrm{RSJ}}(\mathbf{r}, t; \mathbf{r}', t') = \eta(\mathbf{r}, t; \mathbf{r}', t')$ is defined at each bond in the lattice with Gaussian properties $\langle \eta(\mathbf{r}, t; \mathbf{r}', t') \rangle = 0$ and $\langle \eta(\mathbf{r}, t; \mathbf{r} + \mathbf{e}_i, t') \eta(\mathbf{r}', t; \mathbf{r}' + \mathbf{e}_j, t') \rangle = 2T \delta_{i,j} \delta(\mathbf{r} - \mathbf{r}') \delta(t - t')$, where $\mathbf{e}_j$ is a unit vector along the jth direction, and T is the dimensionless temperature.

The TDGL model is defined by taking $\Gamma_{\mathrm{TDGL}}(\mathbf{r}, \mathbf{r}') = \Gamma \delta(\mathbf{r} - \mathbf{r}')$ $(\Gamma = 1)$, and $W_{\mathrm{TDGL}}(\mathbf{r}, t; \mathbf{r}', t') = \eta(\mathbf{r}, t) \delta(\mathbf{r} - \mathbf{r}') \delta(t - t')$; here the noise is also white and defined at each island, with $\langle \eta(\mathbf{r}, t) \rangle = 0$ and $\langle \eta(\mathbf{r}, t) \eta(\mathbf{r}', t') \rangle = 2T \delta(\mathbf{r} - \mathbf{r}') \delta(t - t')$. This model has been used before to study the critical dynamics of the XY model. This is in part because it is computationally less demanding than the RSJ model, which needs time consuming matrix inversions to evaluate $G(\mathbf{r}, \mathbf{r}')$. We find that the macroscopic thermodynamic properties, like the helicity modulus and the phase correlation functions described below, are essentially the same for both models. However, as we show here, other dynamical equilibrium properties are different for the two models, and much more so the out-of-equilibrium quantities [17].

An important aspect of the Shaw *et al.* [9] study is that the SQUID used for measurements was smaller than the array size. The SQUID measures the average net number of thermally nucleated and annihilated vortices that randomly enter or exit its effective area. We do exactly the same in our calculations, by considering regions of the lattice smaller in size than that of the full array simulated [see Fig. 1(b)]. The space-time local vorticity at plaquette $\mathbf{R}$ is defined by $2\pi n(\mathbf{R}, t) = \sum_{\mathcal{P}(\mathbf{R})} [\theta(\mathbf{r}, t) - \theta(\mathbf{r}', t)] \bmod (2\pi)$. Here $\mathcal{P}(\mathbf{R})$ denotes an anticlockwise sum around plaquette $\mathbf{R}$. We imposed periodic boundary conditions (PBC) in both directions in our equilibrium calculations. The average vorticity for the ith SQUID of area $\ell \times \ell$ is defined as $N_\ell^i(t) = \sum_{\mathbf{R} \epsilon (\ell \times \ell)_i} n(\mathbf{R}, t)$. To get the net flux noise we average over all the i-SQUIDs that can be fitted in the array of size $L \times L$ [see Fig. 1(d)]. The flux noise produced by the vortices in the time domain is then generally defined by

$$g_\ell^V(t) \equiv \frac{1}{N_\ell} \sum_i [\langle N_\ell^i(t) N_\ell^i(0) \rangle - \langle N_\ell^i(0) \rangle^2]. \qquad (2)$$

Here N_ℓ is the total number of i-SQUIDs of size $\ell \times \ell$, and the averages $\langle , \rangle$ are carried out over the probability distribution for the noise or over time. Based on the ergodic theorem, both averaging methods should and do give the same results, but the latter is easier to implement numerically. The experimentally measured flux noise is simply given by the Fourier transform of $g_\ell^V(t)$, i.e., $S_\Phi(\omega) = \int dt\, e^{i\omega t} g_\ell^V(t)$. To analyze the scaling results for S_Φ we also need to calculate the time-dependent equilibrium phase correlation function, defined as $g_\theta(\mathbf{r}, \mathbf{r}', t, t') = \langle e^{i[\theta(\mathbf{r}, t) - \theta(\mathbf{r}', t')]} \rangle$. In our explicit calculations we evaluate the zeroth-momentum correlation function, which is known to have only one dominant Lyapunov exponent [18]. Here we concentrate on the $T_{\mathrm{BKT}} < T$ region, as was done in the Shaw *et al.* [9] experiment. In the long distance regime

$$g_\theta(r) = A r^{-\eta} e^{-r/\xi(T)}, \qquad (3)$$

where the correlation length ξ is expected to have the BKT form,

$$\xi(T) = \xi_0 e^{b/\sqrt{T - T_{\mathrm{BKT}}}}, \qquad (4)$$

with T_{BKT}, ξ_0, and b constants determined in the calculations. In Fig. 1 we show the results for the equilibrium time-averaged $g_\theta(r)$ for different temperatures, for both the TDGL (a) and RSJ (c) models in a 64×64 array. In the insets we plot the corresponding $\xi(T)$ data obtained from the correlation function calculations, together with their BKT-type fits. The fitting parameters are $\xi_0 = 0.230(1)$, $b = 1.45(1)$, and $T_{\mathrm{BKT}} = 0.935(1)$ [inset in Fig. 1(a) TDGL] and $\xi_0 = 0.274(30)$, $b = 1.41(10)$, and $T_{\mathrm{BKT}} = 0.917(10)$ [inset in Fig. 1(c) RSJ]. These

nonuniversal results compare well with the numbers obtained from a more extensive Monte Carlo (MC) calculation that gave $\xi_0 = 0.205$, $b = 1.6113$, and $T_{\mathrm{BKT}} = 0.9035$ [18]. The reasonable agreement between these and the MC results gives strong support to the reliability of our dynamic simulation algorithms [19].

The results for $g_\ell^V(t)$ are shown in Figs. 1(b) (TDGL) and 1(d) (RSJ), for an $\ell = 32$ SQUID. As in the experiment we have restricted the analysis to the temperature regime with short correlation lengths in the range $\xi < \ell < L$. We tried different reasonable fitting functions for the data for $g_\ell^V(t)$ in the short and intermediate time regimes, from stretched exponentials, which gave reasonable results, to a novel and somewhat comparable fit, with fewer parameters, which involves the modified Bessel function $K_\nu(t)$, with ν close to zero. The motivation for using the latter functions will become clearer below. First we show the noise functions $S_\Phi(\omega)$ in Fig. 2 (TDGL) (a) and (RSJ) (c). These figures were obtained from a direct fast Fourier transform of the $g_\ell^V(t)$ data. We see there that the intermediate frequency regime of S_Φ can be approximately fitted by a straight line leading to $S_\Phi \sim 1/\omega^{\alpha(T)}$. The α exponent has a weak nonmonotonic temperature dependence but within a rather narrow range, $0.85 \leq \alpha(\mathrm{TDGL})(T) \leq 0.95$, and $1.17 \leq \alpha(\mathrm{RSJ})(T) \leq 1.27$, as shown in the inset of Figs. 2(a) and 2(c). At lower frequencies there is a bending of S_Φ tending towards a flat behavior for the lower temperatures considered. We note that the TDGL α values are closer to the experimental values which were about 1. Although the RSJ results have slightly larger α's they can still be classified as anomalous $1/\omega$ noise. Based on these results we propose an analytic ansatz for $S_\Phi(\omega)$ of the form $S_\Phi(\omega) \sim |\Omega^2 + \omega^2|^{-\alpha(T)/2}$. Here Ω is a characteristic frequency which in our calculations appears to be small. Further justification for this ansatz will be given below. We can then obtain the corresponding expression for $g_\ell^V(t)$ from the inverse Fourier transform of the ansatz for $S_\Phi(\omega)$, giving

$$g_\ell^V(t) = Ct^\nu \frac{\Gamma(1/2)}{\Gamma(\nu + 1/2)} K_\nu(\Omega t), \tag{5}$$

where $\nu \equiv [\alpha(T) - 1]/2$, $\Gamma(x)$ is the gamma function, and C is a constant. We have used this result to fit the numerical data for g_ℓ^V and the fits are shown as continuous lines in Figs. 1(b) and 1(d). Note that based on the calculated values for α, the Bessel function index ν takes the values, $-0.075 \leq \nu(\mathrm{TDGL}) \leq -0.025$ and $0.085 \leq \nu(\mathrm{RSJ}) \leq 0.135$ [recall that $K_{-\nu}(x) = K_\nu(x)$]. It is clear that the TDGL model is rather close to the K_0 result, while the RSJ is slightly different. To further understand our numerical results, given that ν is rather close to zero, it is instructive to first consider the case when $\alpha = 1$, which leads to $g_\ell^V \propto K_0(\Omega t) \propto e^{-\Omega t} \int_0^\infty e^{-2\Omega\tau} d\tau [\tau(\tau + t)]^{-1/2}$, with Fourier transform $\propto (\Omega^2 + |\omega|^2)^{-\frac{1}{2}}$. In the limit when $\omega \gg \Omega$, $S_\Phi(\omega) \sim 1/|\omega|$, while in the opposite limit it is a constant and the noise is white, just as in the experiment. The large ω regime corresponds to the logarithmic short time region of $K_0(\Omega t)$, whereas the lower ω regime corresponds to the exponential one. We can go further by looking at the definition of g_ℓ^V given in Eq. (2), which implies a coarse grained $N(t) \sim t^{-1/2} e^{-\Omega t}$ (for $\alpha = 1$). Here we are making use of the ergodic theorem. We can extend the analysis given above to $\nu \neq 0$, which yields $N(t, \nu(T)) \sim t^{-(1/2-\nu)} e^{-\Omega t}$. The evaluation of the time Fourier transform of $\langle N(\tau, \nu(T)) N(\tau + t, \nu(T)) \rangle$ gets us back to our ansatz for $S_\Phi(\omega)$. This is an interesting result that can be interpreted in terms of an incoherent superposition of a series of independent random wave front events produced by the entering and leaving of vortices from the effective SQUID area. The coarse grained events can be assumed to be Poisson distributed in time so as to produce a random pulse train with the explicit time dependence for g^V given above (see Ref. [20]).

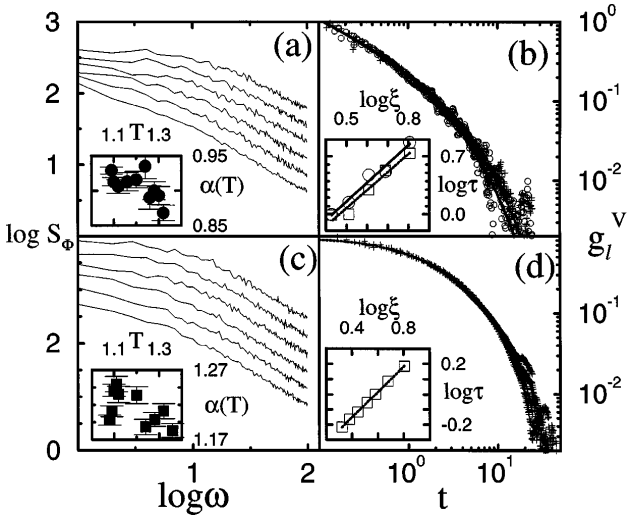

FIG. 2. Flux noise $S_\Phi(\omega)$ vs ω plotted on a log-log scale for TDGL (a) and RSJ (c) dynamics for the same parameters as in Fig. 1. The different temeprature curves have been shifted upwards by a constant distance for clarity. From top to bottom (a) $T = 1.08$, 1.16, 1.24, 1.32, 1.40, and 1.48 and (c) $T = 1.08$, 1.10, 1.12, 1.20, 1.28, and 1.36. In the insets to panels (a) and (c) we plot the exponent $\alpha(T)$ obtained from a least squares fit to the quasilinear frequency regime. The scaling plots for $g_l^V(t)$ are shown in panels TDGL (b) $T = 1.12$, 1.16, 1.20, 1.24, and 1.28), and RSJ (d) ($T = 1.12$, 1.16, 1.20, 1.24, 1.28, 1.32, and 1.36), with $\ell = 16$ (+) and $\ell = 32$ (○). In the insets to panels (b) and (d) we show the scaling of τ_ξ vs ξ on a log-log plot, for $\ell = 32$ (○) and $\ell = 16$ (square). The lines are linear fits to the $\ell = 32$ and $\ell = 16$ results.

Another important experimental result was the test of the dynamic scaling predictions in frequency space. We have carried out an equivalent scaling analysis in time. The general dynamic scaling hypothesis assumes that $g_\ell^V = \xi^\beta F_\ell(t/\tau_\xi, L/\xi, \ell/\xi)$. We find that, as in the experiment, for $\xi < \ell < L$, we can collapse the data into a single curve by considering only the time dependent part of the scaling function, i.e., $g_\ell^V \propto \xi^\beta G(t/\tau_\xi)$, with β an exponent and the relaxation time $\tau_\xi \propto \xi^z$, thereby

defining the dynamical critical exponent, z. We simulated a 64×64 array for different temperatures and we were able to collapse all the data into one single curve for different T's and ℓ's using this criterion. The data collapsed correspond to roughly a decade in τ_ξ. We used data for seven different T's with $\ell = 16$ and $\ell = 32$, for $\xi(T) \epsilon [2.2, 8]$. The accessible length scales and time scales are limited by the available computer power. For a given ξ, we used an $L > 8\xi$ lattice and simulated for $100-1000\tau_\xi$. The scaling results are shown in Fig. 2(b) (TDGL) and 2(d) (RSJ). From the scaling analysis we determined z and obtained the values of $z(\mathrm{TDGL}) \sim 2$ and $z(\mathrm{RSJ}) \sim 0.9$, as shown in the insets of Figs. 2(b) and 2(d). The estimated $z(\mathrm{TDGL}) \sim 2$ exponent is consistent with the value obtained in the experiment [9].

We have also made animations of the vortex motions above T_{BKT}. There we see that the dynamics is dominated by vortex clusters formed above T_{BKT}. One can thus link the anomalous values of the α exponents to the anomalous way in which single vortices diffuse through the clusters with anomalous Hurst exponent [21].

In conclusion, we have studied the flux noise in the TDGL and RSJ models with the goal of providing an understanding to the recent interesting experiments by Shaw *et al.* [9]. We find that by following the prescriptions defined in the experiment, both models lead to anomalous vortex dynamics, with the TDGL results being in closer agreement to the experimental ones. It is possible that the actual samples that are made of large area Nb islands deposited on a copper substrate have a very small resistance to ground and thus the TDGL component may dominate the bond or RSJ term [22]. We also have studied the effect of a small magnetic field and we find that the results change significantly. The α exponent acquires a stronger temperature dependence. Furthermore, we have preliminary results for the $T < T_{\mathrm{BKT}}$ regime and the α values obtained are also indicative of anomalous vortex dynamics. We will report on these and other results in a separate publication.

We thank T. Shaw for a copy of Ref. [9] prior to publication, for careful reading of this Letter, and for several useful informative exchanges. This work was supported in part by the Dutch organization for fundamental research (FOM), by NSF Grant No. DMR-9521845 (J. V. J.) and by the Bavarian "FORSUPRA" program (T. J. H.).

*Present address: Center for the Interdisciplinary Research on Compex Systems, Northeastern University, Boston, MA 02115.

[1] J. M. Kosterlitz and D. J. Thouless, J. Phys. C **6**, 1186 (1973); J. M. Kosterlitz, J. Phys. C **7**, 373 (1974); V. L. Berezinskii, Zh. Teor. Fiz. **61**, 1144 (1971) [Sov. Phys. JETP **32**, 493 (1971)].
[2] J. V. José *et al.*, Phys. Rev. B **16**, 1217 (1977).
[3] D. J. Bishop and J. D. Reppy, Phys. Rev. B **22**, 5171 (1980).
[4] M. R. Beasley *et al.*, Phys. Rev. Lett. **42**, 1165 (1979); A. F. Hebard and A. T. Fiory, *ibid.* **44**, 291 (1980).
[5] D. J. Resnick *et al.*, Phys. Rev. Lett. **47**, 1542 (1981); R. F. Voss and R. A. Webb, Phys. Rev. B **25**, 3446 (1982); D. W. Abraham *et al.*, *ibid.* **26**, 5268 (1982).
[6] Ch. Leemann *et al.*, Phys. Rev. Lett. **56**, 1291 (1986).
[7] V. Ambegaokar *et al.*, Phys. Rev. B **21**, 1806 (1980); S. Doniach and B. A. Huberman, Phys. Rev. Lett. **42**, 1169 (1979).
[8] P. Minnhagen, Rev. Mod. Phys. **59**, 1001 (1987); M. Wallin, Phys. Rev. B **41**, 6575 (1990).
[9] T. J. Shaw *et al.*, Phys. Rev. Lett. **76**, 2551 (1996).
[10] These arrays have zero capacitances, thus zero quantum fluctuations.
[11] Ph. Lerch *et al.*, Helv. Phys. **65**, 389 (1992).
[12] A preliminary version of this work was presented in P. Tiesinga *et al.*, Bull. Amer. Phys. Soc. **41**, 466 (1996).
[13] For a recent review, see, for example, D. Domínguez and J. V. José, Int. J. Mod. Phys. B **8**, 3749 (1994), and references therein.
[14] R. Loft and T. A. De Grand, Phys. Rev. B **35**, 8528 (1987); A. N. Pargellis *et al.*, Phys. Rev. E **49**, 4250 (1994).
[15] H. Beck, Phys. Rev. B **49**, 6153 (1994).
[16] A. Jonsson and P. Minnhagen, Phys. Rev. Lett. **73**, 3576 (1994); J. Houlrik *et al.*, Phys. Rev. B **50**, 3953 (1994); P. Minnhagen and O. Westman, Physica (Amsterdam) **220C**, 347 (1994).
[17] We have found, for example, that the single vortex viscosity in the RSJ model is nonlinear in velocity [see T. J. Hagenaars *et al.*, Phys. Rev. B **50**, 1143 (1994)], while it is linear in the TDGL model. This difference may be important to explain the differences in the critical exponents for both models.
[18] G. Ramirez-Santiago and J. V. José, Phys. Rev. Lett. **68**, 1224 (1992); Phys. Rev. B **49**, 9567 (1994).
[19] H. Eikmans and J. E. van Himbergen, Phys. Rev. B **41**, 8927 (1990); D. Domínguez *et al.*, Phys. Rev. Lett. **67**, 2367 (1991).
[20] H. Schoenfeld, Z. Naturforsch. Teil A **10**, 291 (1955); see also M. J. Bukingham, *Noise in Electronic Devices and Systems* (Ellis Horwood Limited Publishers, Chichester, West Sussex, England, 1983).
[21] For a review and further related references, see J. Feder, *Fractals* (Plenum Press, New York, 1988).
[22] T. J. Shaw (private communication).